Large Scale Production of Continuous Hydrogel Fibers with Anisotropic Swelling Behavior by Dynamic-Crosslinking-Spinning

Kai Hou, Huiyi Wang, Yunyin Lin, Shaohua Chen, Shengyuan Yang, Yanhua Cheng, Benjamin S. Hsiao, Meifang Zhu*

Hydrogel microfibers have been considered as a potential biomaterial to spatiotemporally biomimic 1D native tissues such as nerves and muscles which are always assembled hierarchically and have anisotropic response to external stimuli. To produce facile hydrogel microfibers in a mathematical manner, a novel dynamic-crosslinking-spinning (DCS) method is demonstrated for direct fabrication of size-controllable fibers from poly(ethylene glycol diacrylate) oligomer in large scale, without microfluidic template and in a biofriendly environment. The diameter of fibers can be precisely controlled by adjusting the spinning parameters. Anisotropic swelling property is also dependent on inhomogeneous structure generated in spinning process. Comparing with bulk hydrogels, the resulting fibers exhibit superior rapid water adsorption property, which can be attributed to the large surface area/volume ratio of fiber. This novel DCS method is one-step technology suitable for large-scale production of anisotropic hydrogel fibers which has a promising application in the area such as biomaterials.

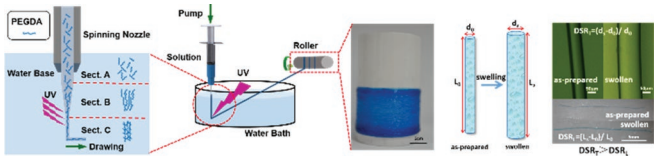

1. Introduction

Tissues are mostly formed with hierarchical structures to enable specific functions in vivo. In human body, many types of fibrous tissues such as blood vessel,[1] muscle cells,[2] and nerves,[3] are playing important roles in maintaining body functions.[4] In recent years, various fibrous biomaterials, including nanofibers,[5] fibrous composites,[6] and fiber mats,[7] have been engineered to mimic the hierarchical structures of fibrous tissues biologically. Hydrogel is a common biomaterial due to its high water retention property, easy to be functionalized, pore size controllable, and stimuli-responsive property, etc.[8] where hydrogel microfibers have become an important class of hydrogel materials for cell scaffolds and artificial tissues due to the following reasons. First, hydrogel microfibers have suitable size to mimic the microscale fibrous structure of tissues such as nerve cells (≈10^1 μm)[9] and muscle fibers (≈10^1–10^2 μm).[10] Second, complex native tissues are always assembled from low dimension materials to complicated structural arrangement hierarchically.[4c,11] In other words, fiber-shaped materials can be utilized in the reconstruction of specific 3D structures which are necessary for tissue remodeling. Third, the surface area/volume ratio (SA:V) of hydrogel fibers is inherently large so that

K. Hou, H. Wang, Y. Lin, Dr. S. Chen, Dr. S. Yang, Dr. Y. Cheng, Prof. M. Zhu
State Key Laboratory for Modification of Chemical Fibers and Polymer Materials
College of Materials Science and Engineering
Donghua University
2999 North Renmin Road, Shanghai 201620, P. R. China
E-mail: zhumf@dhu.edu.cn
Prof. B. S. Hsiao
Department of Chemistry
Stony Brook University
Stony Brook, NY 11794, USA

DOI: 10.1002/marc.201600430

these materials can promote the nutrients transportation and spatial distribution of cells.[12]

Several techniques have been established to fabricate hydrogel microfibers, including electrospinning, extrusion, ink-jet printing, wet spinning, and microfluidic template. Electrospinning has been adopted as a popular method to fabricate hydrogel fibers.[13] However, it merely produces nonwoven fiber mats and the residual organic solvents are always incompatible with bioenvironment. Extrusion is one of the most common methods,[2a] but it is not suitable when the highly cross-linked polymers are used as the raw materials. Ink-jet printing can fabricate complex and delicate patterns but the instruments utilized during the fabricating process are complex.[14] Wet spinning is one of the most convenient methods to produce large scale hydrogel fibers from natural[15] and synthetic[16] polymers. However, the polymers suitable for wet spinning are required to have appropriate structure and molecular weight. What is more, fibers fabricated from natural materials, such as calcium alginate, have been proved unstable in vivo due to its tendency to dissolve in typical ionic conditions of human body.[17] Additionally, the solvents utilized to produce chemical fibers through wet spinning are usually toxic and not biocomfortable. Recently, coaxial based microfluidic technique has been demonstrated to fabricate hydrogel microfibers with specific size and shapes.[18] For example, polymers like poly(lactic-*co*-glycolic acid) (PLGA)[19] and alginate[20] have been used to fabricate hydrogel fibers via microfluidic technique successfully, where oligomers and monomers are also applicable.[12] During the fabrication process, gelation of hydrogel fibers occurred inside the microfluidic channels, where the gelation rate could be regulated by controlling solidification conditions that was vital for the continuous production of fibers in a multiphase coaxial flow. But this method was difficult to produce uniform fibers in large-scale conveniently due to the complex structure of microfluidic template.

Suitable fibrous biomaterials must have a fibrous shape and anisotropic property to mimic nature tissues with anisotropic response to external stimuli such as muscle contraction or neural signaling.[14a] However, anisotropic hydrogel fibers were hardly fabricated and the structure was mainly based on asymmetric structure such as multilayers via microfluidic templates technique.[21] Here, a simplified approach has been demonstrated to produce hydrogel microfibers with anisotropic property on a large scale. In specific, we developed a novel dynamic-crosslinking-spinning (DCS) method for facile fabrication of size-controllable hydrogel fibers from poly(ethylene glycol diacrylate) (PEGDA) oligomer without any microfluidic template. The diameter of fibers can be precisely controlled by spinning parameters. Interestingly, the resulting fibers exhibited anisotropic swelling behavior which might be dependent on the inhomogeneous structure generated by drawing force in spinning process. This anisotropic swelling behavior and high water retention property were both related with the spinning conditions. We also demonstrated that, compared with bulk hydrogels, the obtained hydrogel fibers exhibited superior and rapid water adsorption properties which are due to the large surface area/volume ratio of fiber. In summary, the novel DCS technology can provide a one-step method for large-scale production of anisotropic hydrogel fibers that can be used in a wide range of biomedical applications.

2. Experimental Section

2.1. Materials

PEGDA (M_n = 700) and photoinitiator 2-hydroxy-4′-(2-hydroxyethoxy)-2-methylpropiophenone (IRGACURE 2959, I2959, 98%) were purchased from Sigma-Aldrich. $CDCl_3$ was purchased from J&K Scientific Ltd. Karl-Fisher solution (pyridine-free) was obtained from Sinopharm Chemical Reagent Co., Ltd. Deionized water was supplied by a water purification system (Heal Force Bio-Meditech Holdings Ltd).

2.2. Fabrication of PEGDA Hydrogel Fibers

A mixture of I2959 and PEGDA (I2959:PEGDA = 5:1000, wt%) was dissolved in deionized water to produce different concentrations of solutions under continuous magnetic stirring in the dark. These solutions were subsequently utilized for DCS.

In a typical process, the spinning solution was extruded into a water bath by a metering pump (KDS100, KD Scientific, USA). And the photopolymerization of the extruded flow was initiated under water by mercury lamp UV irradiation (S1500, EXFO, Canada, λ = 360 nm, 2.77 W cm^{-2}) which resulted in a continuous hydrogel fiber. A custom-built fiber collection system with adjustable winding speed of 0–1000 m h^{-1} applied drawing force to reduce the diameter of fibers. The fiber was collected on a plastic roller outside the bath.

Bulk hydrogels were also prepared as a control and photopolymerized in a 50 mm (long) × 6 mm (diameter) cylindrical glass tube from the same solutions as hydrogel fibers.

2.3. Characterization of Hydrogel Fibers

The rheology of the spinning solutions was determined by a rotational rheometer (50 mm plate mode, ARES, TA, USA). ^{13}C NMR spectra were recorded on a NMR spectrometer (Bruker Avance-400 MHz, Swiss). Fourier transform infrared (FTIR) spectra were obtained by a Fourier transform infrared spectrophotometer (Nicolet 6700, Thermo Fisher, USA, wavenumber ranged from 4000 to 600 cm^{-1}). The as-prepared hydrogel fibers were soaked in pure water for 24 h in order to remove impurities and then lyophilizated for solid state NMR and FTIR spectra detection. In addition, PEGDA oligomer was dissolved in $CDCl_3$ for liquid NMR characterization. The morphology of hydrogel fibers was

observed by scanning electron microscopy (SEM, JSM-5600LV, Nippon-Optical, Japan) and stereoscopic microscopy (SMZ745T, Nikon, Japan). Diameters of the fibers were measured by optical microscopy (VHM2600, VIHENT, China), and the mean values of ten fibers were reported.

Water retention (*WR*) of fibers was detected by a Karl-Fischer coulomb titration system (MA-1, BENON, China), which was a traditional method for moisture detection of microsize gel.[22] *WR* of bulk hydrogels was calculated by the equation below

$$WR = \frac{W_t - W_d}{W_d} \times 100\% \quad (1)$$

where W_t was the real-time weight of hydrogel, W_d was the dry weight of as-prepared hydrogel.

Dimensional swelling ratio on transverse direction (DSR_T) and longitudinal direction (DSR_L) were, respectively, calculated by the following equations[14a]

$$DSR_T = \frac{d_s - d_o}{d_o} \times 100\% \quad (2)$$

$$DSR_L = \frac{L_s - L_o}{L_o} \times 100\% \quad (3)$$

where d_s and L_s were the dimension of equilibrium swollen hydrogels or fibers on transverse and longitudinal direction, respectively, d_0 and L_0 were the dimensions of as-prepared hydrogels or fibers on transverse and longitudinal direction, respectively.

3. Results and Discussion

3.1. Fabrication and Morphology of Hydrogel Fibers

The schematic illustration of DCS is shown in Figure $1A_1$. In this process, the PEGDA solution did not dissolve immediately when extruded into water (Figure $1A_1$ Sect. A), but formed a fiber-shape aggregate due to the viscoelasticity of the PEGDA solution (Figure S1, Supporting Information). This PEGDA phase could not be drawn and collected as a fiber which was due to that the molecular chain of PEGDA monomer is short and interaction among monomers is weak. In order to make the monomer rapidly polymerized, which is important to form cross-linked structure and maintain the fiber shape during extrusion instantaneously, the UV irradiation was utilized because the photopolymerization process can complete in less than 1 s.[18a] As a result, the PEGDA monomer phase was solidified and a continuous fiber could be formed along with the extrusion of the solution dynamically (Figure $1A_1$ Sect. C). Meanwhile, a roller was used for fiber collection and provided the drawing force to reduce the fiber diameter. We observed that the drawing region (Figure $1A_1$ Sect. B) took place before the UV irradiation point, which was due to the fact that the formed cross-linked structure (Figure $1A_1$ Sect. C) limits the hydrogel network deformation.[23] In contrast, the oligomer solution stream (Figure $1A_1$ Sect. B) had better flowability, so that could be drawn thinner.

^{13}C NMR and FTIR spectra were performed to determine the degree of polymerization after the dynamical cross-linking process.[24] The ^{13}C NMR spectra result (Figure S2A, Supporting Information) showed that the polymerization occurred between C=C double bond. However, as the FTIR spectra show (Figure S2B, Supporting Information), there were residual acrylate groups after polymerization. Comparing with in situ polymerization, the drawing force in DCS process as dynamic fluctuations may cause the distance among oligomer becoming larger in the process of cross-linking, which results in isolated acrylate groups and nonuniform structure of fiber after polymerization.[26b]

Fiber could be continuously and regularly collected by a roller on a large scale as Figure $1A_2$ illustrates. The solution was dyed for clarity by adding 2 wt% methylene blue. The dimensional homogeneity and surface morphology of hydrogel fibers are shown in Figure 1B by scanning electron microscope. Figure $1B_1$ illustrates the alignment of fiber yarns. The diameter of fibers was uniform which confirmed that this nontemplate method can fabric hydrogel fiber uniformly and steadily. Figure $1B_2$,B_3 shows surface morphology of fiber in different magnifications. The wrinkle was observed on the surface of fiber which was attributed to the internal pore collapse caused by lyophilization.[12] In addition, woven structure can be obtained by a traditional warp–weft knitting technology on a manual device. As Figure $1C_1$ illustrates, nylon fibers were set as warp, and hydrogel fibers weft was shuttled through warp which were separated by raising and heddles repeatedly. Figure $4C_2$,C_3 is the photo and SEM image of the 2D hydrogel fabric, respectively. The arrangement of hydrogel weft is orderly and compact to ensure that the woven structure is stable. This woven structure suggests that hydrogel fibers have the potential on the multiscale structure reconstruction to expand the applications of this material.

The results confirmed that uniform and continuous hydrogel fibers could be obtained through this novel nontemplate DCS method by using low molecular weight oligomer as raw materials. Moreover, the drawing force in the DCS method was not only for fiber collection, but could also be used to control the diameter of fibers which will be discussed next.

3.2. Diameter Control of Hydrogel Fibers

Groups of hydrogel fibers under different concentrations (C_{PEGDA}), extrusion rate (E_r), and winding speed (V_w) conditions were prepared and then the relationships between the fiber diameter and processing parameters were analyzed. The results are summarized in Figure 2. It reveals that the square of diameter (d^2) of hydrogel fibers

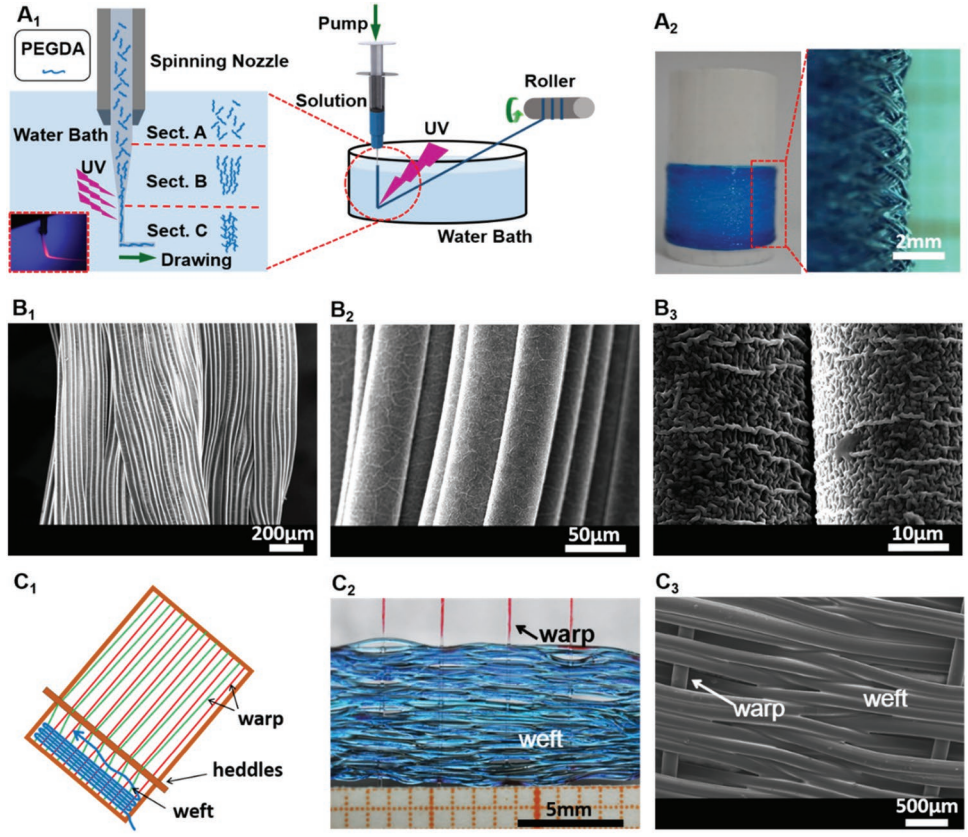

Figure 1. Fabrication of hydrogel fibers. A_1) Schematic illustration of the dynamic-crosslinking-spinning. Enlarged schematic shows the polymerization process under drawing force. Insert is the photo of enlarged schematic (dyed by Rhodamine B). A_2) Photos of hydrogel fibers (dyed by methylene blue) on a plastic roll. B_1–B_3) SEM images of a bundle of the hydrogel fibers in different magnifications. C_1–C_3) Woven schematic illustration of fibers and images of the hydrogel textile (nylon as warp and hydrogel fiber as weft).

was almost linearly influenced by C_{PEGDA} (Figure 2A), E_r (Figure 2B), and $1/V_w$ (Figure 2C). An experimental relationship could be deduced as below

$$d^2 \propto C_{PEGDA} \times E_r / V_w \tag{4}$$

In addition, a deformation relationship could be obtained below by introducing a constant π and a variant t (spinning time)

$$\left(\frac{d^2\pi}{4}\right) \times V_w \times t \propto C_{PEGDA} \times E_r \times t \tag{5}$$

where $\left(\frac{d^2\pi}{4}\right) \times V_w \times t$ represents the total volume of fibers collected, and $C_{PEGDA} \times E_r \times t$ is the total amount of PEGDA oligomer extruded. This indicates that the volume of fibers collected is linearly influenced by the total amount of PEGDA oligomer extruded. Comparing with the microfluidic template method, the demonstrated DCS method is an effective nontemplate technique which could produce fibers with precisely controlled size by adjusting the spinning conditions. In addition, this DCS process was accompanied with simultaneous swelling behavior which will be discussed next.

3.3. Swelling Behavior of Hydrogel Fibers

In order to investigate the swelling behavior that occurred in the DCS process, *WR* of as-prepared fibers was detected and the results are shown in Figure 3A. It indicates that there is an intersection point between the water retention of solutions (WR_S) and that of as-prepared fibers (WR_f). The WR_f was linearly influenced by the concentration of spinning solution (C_{PEGDA}). Before C_{PEGDA} reached the point, WR_f was lower than WR_S. The possible reason is that, when C_{PEGDA} was low, the space among neighboring oligomer was large which shrank after photopolymerization because of the formed covalent bond shortened distance between two oligomers.[25] As a result, water was squeezed out of the polymer matrix in the spinning process. Reversely, when C_{PEGDA} was higher than the concentration at this point, water was more likely to diffuse into the polymer matrix due to the concentration gradient, and this difference value

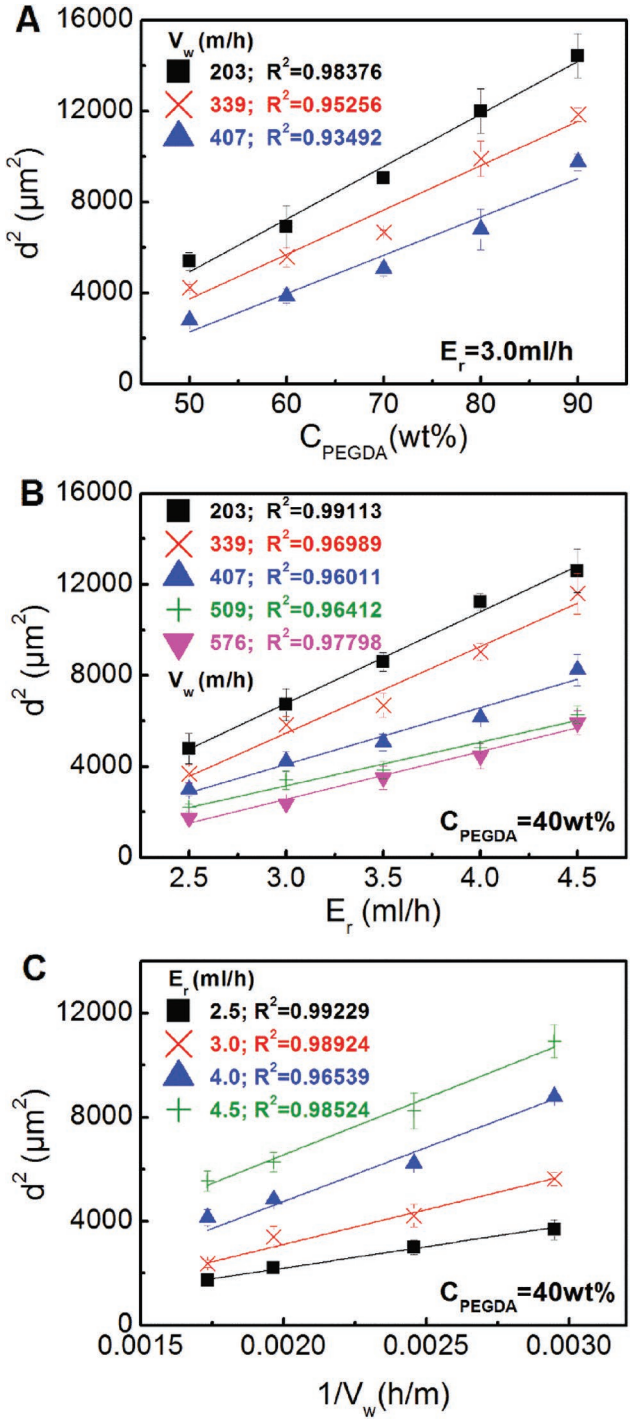

Figure 2. Dependence of the diameters of the hyrogel fibers on the A) concentration of the spinning solution (C_{PEGDA}), B) the extrusion rate (E_r), and C) winding speed (V_w).

became larger when C_{PEGDA} increased. Moreover, the gap between water retention of equilibrium swollen fibers (WR_e) and as-prepared fibers (WR_f) increased when C_{PEGDA} became higher. In addition, the influence of the winding speed (V_w) on WR_f was also investigated. As Figure 3B shows, the WR_f was almost not affected by the increased V_w. This result indicates that swelling behavior occurred in the DCS process synchronously and WR_f was only affected by C_{PEGDA}. One possible explanation is that the formed cross-linked structure has lower deformation ability which limited water to be squeezed out of fibers matrix under the drawing force applied. In specific, the WR_e was logarithmically influenced by V_w. It is conceivable that the increasing drawing force applied on PEGDA stream (Figure 1A Sect. B) may cause the disentanglement among PEGDA chains. With the increasing of the drawing force, the distance among PEGDA oligomers became larger which resulted in larger space among the cross-linking points and finally caused higher WR_e of hydrogel fibers. However, the precise reason is under investigation.

Figure 3C shows the water retention curves of the hydrogel fibers. In comparison, the water retention of bulk hydrogel was also determined under the same conditions as control and the result is shown in Figure S3 (Supporting Information). It is noted that the hydrogel fibers exhibited faster water adsorption than the bulk hydrogels. The time to reach the equilibrium swelling for hydrogel fibers was in 20 s, almost 3600 times faster than that of bulk hydrogels because the SA:V of 1D material is much larger than that of 3D material.[19,20] The rapid water absorption rate and excellent overall property of hydrogel fibers are very important for the nutrient diffusion in tissue as biomaterials.

Finally, we found that the fibers produced by DCS process exhibited anisotropic swelling behavior. Different from bulk hydrogels, whose dimensional swelling ratios on the transverse direction (DSR_T) and longitudinal direction (DSR_L) are nearly identical (Figure S4, Supporting Information), DSR_T is much large than DSR_L (Figure 4A) for hydrogel fibers. The relationships between $\frac{DSR_T}{DSR_L}$ and the spinning parameters were also investigated. Figure 4B shows that DSR_T decreased with the reduction of concentration (C_{PEGDA}), where DSR_L exhibited two stages of changes when C_{PEGDA} increased, i.e., DSR_L increased first and decreased subsequently. As a result, $\frac{DSR_T}{DSR_L}$ showed a parabola trend with the increase of C_{PEGDA} (inset of Figure 4B). In addition, we found that the faster winding speed (V_w) could lead to decreases of DSR_T and DSR_L simultaneously (Figure 4C), but V_w did not affect the ratio of $\frac{DSR_T}{DSR_L}$ obviously (inset of Figure 4C). Comparing with the homogeneous structure formed in the static polymerization process of bulk hydrogels, inhomogeneous structure is thought to form due to the stable drawing force in the DCS process which probably resulted in the unique swelling behavior.[26] However, the mechanism of this anisotropic swelling behavior which clearly correlated

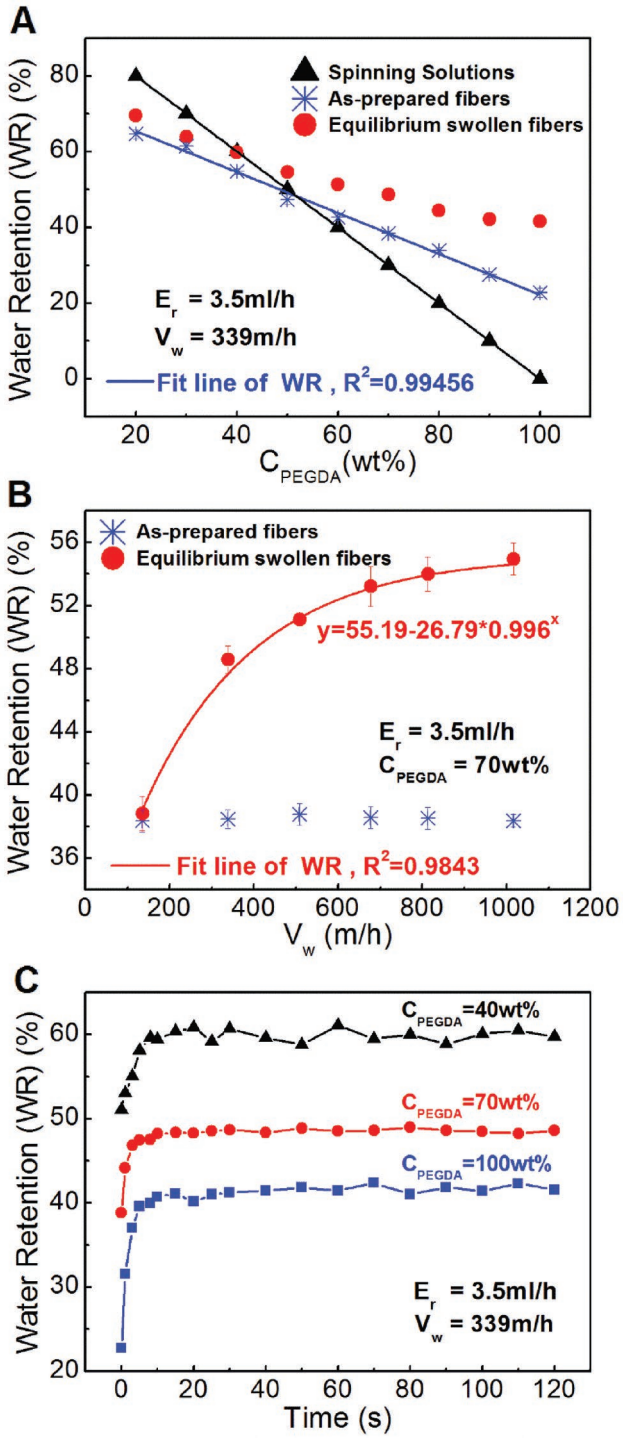

Figure 3. Dependence of the water retention (*WR*) property of the hydrogel fibers on the A) concentration of the spinning solution (C_{PEGDA}) and B) winding speed (V_w). C) *WR* curves of the hydrogel fibers.

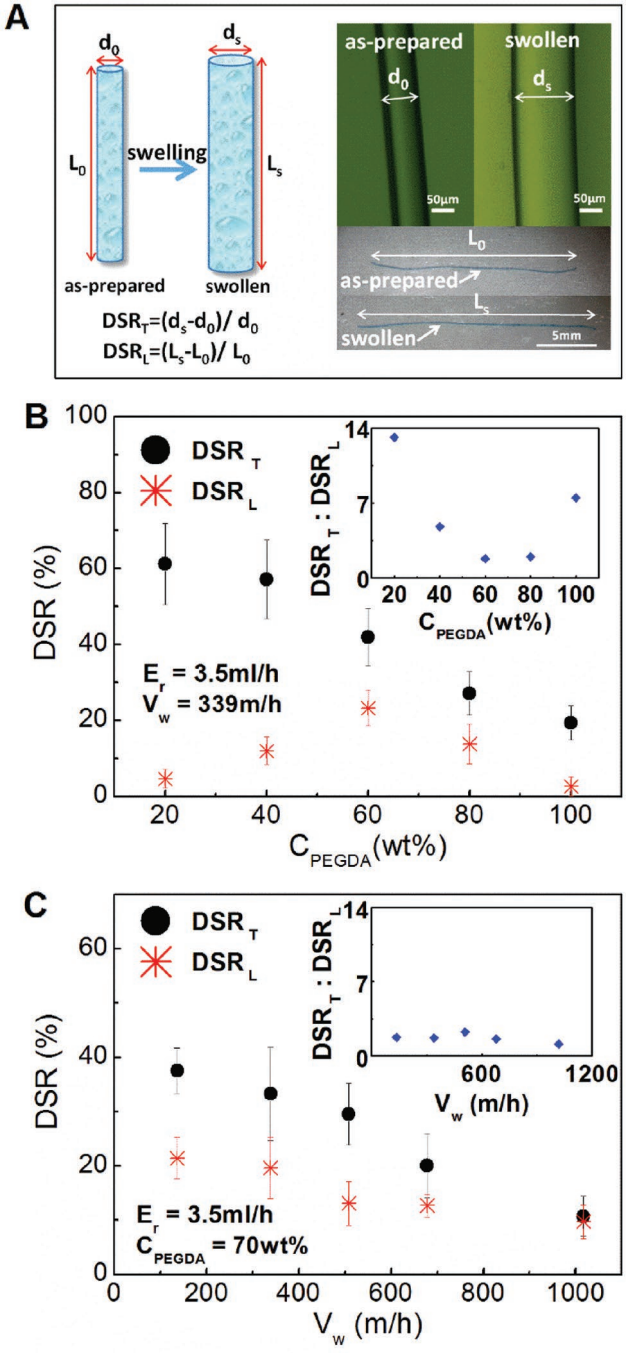

Figure 4. Anisotropic swelling behavior of hydrogel fibers. A) Schematic illustration and photos of anisotropic dimension swelling ratio (*DSR*) of hydrogel fibers; Scale bar of DSR_T and DSR_L images are 50 μm and 5 mm, respectively. Dependence of dimension swelling ratio of the hydrogel fibers on the B) concentration of the spinning solution (C_{PEGDA}) and C) winding speed (V_w).

with the spinning parameters is still not known. A more in-depth study on the formation and evolution of the condensed state and cross-linked structure of hydrogel fibers need to be investigated further.

4. Conclusions

In summary, in order to realize the large-scale production of hydrogel microfibers, a novel nontemplate DCS method

has been developed that can fabric continuous and uniform hydrogel fibers from low molecular weight oligomer PEGDA. The diameter of the hydrogel fibers can be precisely controlled by the concentration of solution (C_{PEGDA}), extrusion rate (E_r), and winding speed (V_w). The resultant hydrogel fibers exhibited superior rapid water adsorption property which can be attributed to their large surface area/volume ratio. In addition, hydrogel fibers exhibited anisotropic swelling behavior and outstanding water retention property that can be controlled by the spinning parameters. These hydrogel fibers could be further weaved by typical textile instruments providing us new materials for reconstruction of hierarchical multistructured devices with considerable application opportunities in the area such as biomaterials.

Supporting Information

Supporting Information is available from the Wiley Online Library or from the author.

Acknowledgements: This research was financially supported by the Program for Changjiang Scholars and Innovative Research Team in University (T2011079, IRT1221) and the Research Program of the Shanghai Science and Technology Commission (13NM1400102).

Received: July 8, 2016; Revised: August 29, 2016; Published online: October 14, 2016; DOI: 10.1002/marc.201600430

Keywords: anisotropic swelling; biomaterials; hydrogel; hydrogel fibers; rapid swelling

[1] a) B. C. Isenberg, C. Williams, R. T. Tranquillo, *Circ. Res.* **2006**, *98*, 25; b) L. Soletti, A. Nieponice, J. Guan, J. J. Stankus, W. R. Wagner, D. A. Vorp, *Biomaterials* **2006**, *27*, 4863.
[2] a) Y. Li, C. T. Poon, M. Li, T. J. Lu, B. Pingguan-Murphy, F. Xu, *Adv. Funct. Mater.* **2015**, *25*, 5999; b) B. J. Vakoc, R. M. Lanning, J. A. Tyrrell, T. P. Padera, L. A. Bartlett, T. Stylianopoulos, L. L. Munn, G. J. Tearney, D. Fukumura, R. K. Jain, B. E. Bouma, *Nat. Med.* **2009**, *15*, 1219.
[3] a) Y. Wang, F. Qi, S. Zhu, Z. Ye, T. Ma, X. Hu, J. Huang, Z. Luo, *Acta Biomater.* **2013**, *9*, 7248; b) G. T. Christopherson, H. Song, H. Q. Mao, *Biomaterials* **2009**, *30*, 556; c) L. Yao, N. O'Brien, A. Windebank, A. Pandit, *J. Biomed. Mater. Res., Part B* **2009**, *90B*, 483.
[4] a) X. T. Shi, S. Ostrovidov, Y. H. Zhao, X. B. Liang, M. Kasuya, K. Kurihara, K. Nakajima, H. Bae, H. K. Wu, A. Khademhosseini, *Adv. Funct. Mater.* **2015**, *25*, 2250; b) S. Lee, M. K. Leach, S. A. Redmond, S. Y. C. Chong, S. H. Mellon, S. J. Tuck, Z. Q. Feng, J. M. Corey, J. R. Chan, *Nat. Methods* **2012**, *9*, 917; c) H. Onoe, T. Okitsu, A. Itou, M. Kato-Negishi, R. Gojo, D. Kiriya, K. Sato, S. Miura, S. Iwanaga, K. Kuribayashi-Shigetomi, Y. T. Matsunaga, Y. Shimoyama, S. Takeuchi, *Nat. Mater.* **2013**, *12*, 584.
[5] a) X. Jingwei, M. R. MacEwan, S. M. Willerth, L. Xiaoran, D. W. Moran, S. E. Sakiyama-Elbert, X. Younan, *Adv. Funct. Mater.* **2009**, *19*, 2312; b) J. Xie, M. R. MacEwan, W. Z. Ray, W. Liu, D. Y. Siewe, Y. Xia, *ACS Nano* **2010**, *4*, 5027.
[6] A. Hsieh, T. Zahir, Y. Lapitsky, B. Amsden, W. Wan, M. S. Shoichet, *Soft Matter* **2010**, *6*, 2227.
[7] K. M. Schultz, L. Campo-Deano, A. D. Baldwin, K. L. Kiick, C. Clasen, E. M. Furst, *Polymer* **2013**, *54*, 363.
[8] a) A. K. Gaharwar, P. J. Schexnailder, A. Dundigalla, J. D. White, C. R. Matos-Perez, J. L. Cloud, S. Seifert, J. J. Wilker, G. Schmidt, *Macromol. Rapid Commun.* **2011**, *32*, 50; b) R. J. Wade, E. J. Bassin, W. M. Gramlich, J. A. Burdick, *Adv. Mater.* **2015**, *27*, 1356; c) G. C. Ingavle, S. H. Gehrke, M. S. Detamore, *Biomaterials* **2014**, *35*, 3558; d) Y. H. Li, G. Y. Huang, X. H. Zhang, B. Q. Li, Y. M. Chen, T. L. Lu, T. J. Lu, F. Xu, *Adv. Funct. Mater.* **2013**, *23*, 660; e) U. A. Gurkan, Y. T. Fan, F. Xu, B. Erkmen, E. S. Urkac, G. Parlakgul, J. Bernstein, W. L. Xing, E. S. Boyden, U. Demirci, *Adv. Mater.* **2013**, *25*, 1192; f) P. M. Kharkar, K. L. Kiick, A. M. Kloxin, *Chem. Soc. Rev.* **2013**, *42*, 7335.
[9] J. Y. Lee, C. A. Bashur, A. S. Goldstein, C. E. Schmidt, *Biomaterials* **2009**, *30*, 4325.
[10] F. Maier, A. Bornemann, *Muscle Nerve* **1999**, *22*, 578.
[11] M. Akbari, A. Tamayol, V. Laforte, N. Annabi, A. H. Najafabadi, A. Khademhosseini, D. Juncker, *Adv. Funct. Mater.* **2014**, *24*, 4060.
[12] M. A. Daniele, S. H. North, J. Naciri, P. B. Howell, S. H. Foulger, F. S. Ligler, A. A. Adams, *Adv. Funct. Mater.* **2013**, *23*, 698.
[13] M. S. Austero, A. E. Donius, U. G. K. Wegst, C. L. Schauer, *J. R. Soc., Interface* **2012**, *9*, 2551.
[14] a) A. S. Gladman, E. A. Matsumoto, R. G. Nuzzo, L. Mahadevan, J. A. Lewis, *Nat. Mater.* **2016**, *15*, 413; b) T. Billiet, E. Gevaert, T. De Schryver, M. Cornelissen, P. Dubruel, *Biomaterials* **2014**, *35*, 49.
[15] M. Dash, F. Chiellini, R. M. Ottenbrite, E. Chiellini, *Prog. Polym. Sci.* **2011**, *36*, 981.
[16] F. Dini, G. Barsotti, D. Puppi, A. Coli, A. Briganti, E. Giannessi, V. Miragliotta, C. Mota, A. Pirosa, M. R. Stornelli, P. Gabellieri, F. Carlucci, F. Chiellini, *J. Bioact. Compat. Polym.* **2016**, *31*, 15.
[17] Q. Yimin, *Polym. Adv. Technol.* **2008**, *19*, 6.
[18] a) M. A. Daniele, D. A. Boyd, A. A. Adams, F. S. Ligler, *Adv. Healthcare Mater.* **2015**, *4*, 18; b) A. L. Thangawng, P. B. Howell, J. J. Richards, J. S. Erickson, F. S. Ligler, *Lab Chip* **2009**, *9*, 3126.
[19] C. M. Hwang, A. Khademhosseini, Y. Park, K. Sun, S. H. Lee, *Langmuir* **2008**, *24*, 6845.
[20] J. Su, Y. Zheng, H. Wu, *Lab Chip* **2009**, *9*, 996.
[21] a) E. Kang, G. S. Jeong, Y. Y. Choi, K. H. Lee, A. Khademhosseini, S. H. Lee, *Nat. Mater.* **2011**, *10*, 11; b) S. Cho, T. S. Shim, S. M. Yang, *Lab Chip* **2012**, *12*, 3676.
[22] K. Gawlitza, R. Georgieva, N. Tavraz, J. Keller, R. von Klitzing, *Langmuir* **2013**, *29*, 16002.
[23] M. Zhu, Y. Liu, B. Sun, W. Zhang, X. Liu, H. Yu, Y. Zhang, D. Kuckling, *Macromol. Rapid Commun.* **2006**, *27*, 1023.
[24] a) Q. Gao, Z. Y. Qin, C. C. Li, S. F. Zhang, J. Z. Li, *BioResources* **2013**, *8*, 5380; b) Y. Wang, B. Han, R. Shi, L. Pan, H. Zhang, Y. Shen, C. Li, F. Huang, A. Xie, *J. Mater. Chem. B* **2013**, *1*, 6411.
[25] Z. Wei, D. HuaNan, Z. Tao, G. JinBao, W. Jie, *J. Appl. Polym. Sci.* **2012**, *125*, 77.
[26] a) F. Ikkai, M. Shibayama, *J. Polym. Sci., Part B: Polym. Phys.* **2005**, *43*, 617; b) E. S. Matsuo, M. Orkisz, S. T. Sun, Y. Li, T. Tanaka, *Macromolecules* **1994**, *27*, 6791.